PREPARATION OF THE SAMPLE
AND
X-RAY DIFFRACTION STUDY

CHAPTER - II

PREPARATION OF THE SAMPLE AND X-RAY DIFFRACTION STUDY

2.1 Introduction

Most of the ferroelectric compounds with the general formula ABO_3 have the perovskite structure, where A is monovalent or divalent metal and B is a tetra or pentavalent one. The atomic arrangement in this structure was first found for the mineral perovskite $CaTiO_3$.

Potassium niobate ($KNbO_3$) is of the perovskite type ferroelectrics as first reported by Shirane et al (1954). It is particularly interesting to note that potassium niobate is ferroelectric at room temperature. The general characteristics of $KNbO_3$ crystal are expected to be similar to those of $BaTiO_3$. (Refer Table 2.1). Potassium niobate exhibits the cubic porovskite structure (O_h-m3m) above curie temperature 415° and below 415° it transforms successively to three ferroelectric phases, first (C_{4v} - 4mm) tetragonal, then to (C_{2v}- mm) orthorhombic phase at about 224^oC and finally to a (C_{3v}-3m) orthorhombic phase below -12^oC. The polar axis in the three ferroelectrics phases are [001], [011] and [111] respectively (1,2,3,4).

The temperature dependence of the lattice parameters of $KNbO_3$ was studied first by Wood (3) and later, by Shirane et al (1). The general appearance of the curve is again quite similar to the corresponding curve of $BaTiO_3$, but the spontaneous strain in $KNbO_3$ is larger in all three phases. This is not unexpected owing to the fact that the Curie temperature of $KNbO_3$ is higher than that of $BaTiO_3$, and a higher Curie temperature is generally indicative of stronger interactions, nature of these are not yet known clearly.

It is worth mentioning that $KNbO_3$ is the only ferroelectric crystal that exhibits the same phase symmeteries and the same sequence of transitions as $BaTiO_3$. A comparision between the two crystals is given in Table 2.1.

Table 2.1   Comparison between $KNbO_3$ and $BaTiO_3$

	$KNbO_3$	$BaTiO_3$
Transition Temperatures ($^\circ$c)	435,225,-10	120,5,-90
Transition energies (cal/more)	190,85,32	49,21.11
Maximum tetragonal distortion c/a	1.017	1.010
Spontaneous polarization at the curie point (10^{-6} c/m^2)	26	18
Curie constant C($^\circ$k) as defined from $\epsilon = \dfrac{C}{T-T_o}$	2.4×10^5	1.7×10^5
$T_c - T_o$ ($^\circ$C)	58	11
Coefficients ξ_{11}^X and ξ_{111}^X of the free energy expansion $A = \frac{1}{2} \chi^X P^2 + \frac{1}{4} \xi_{11}^X P^4 + \frac{1}{6} \xi_{111}^X P^6$	$\xi_{11}^X = -10 \times 10^{-13}$ c.g.s and $\xi_{111}^X = 54 \times 10^{-23}$ c.g.s	-20×10^{-13} c.g.s and 25×10^{-23} c.g.s.
Orthorhombic to tetragonal Q is the transition heat and S in the transition entropy. Q(calmole^{-1}); }Q }S	85 ± 10 0.17	15-26 .054-.091
Tetragonal to cubic }Q }S	134.5±5 to 190±15 0.19 to 0.27	10 to 50 ± 5 .125

The nuclear quadrupole resonance of Nb^{93} has been studied in all four phases of $KNbO_3$ by Cotts and Knight (7). The results of this experiment yield information of about the field gradient and its asymmetry at the position of the Nb nucleus. The interpretation of the result is the symmetry of the resonance lines can be used as a sensitive detector of the different phase transitions. The result that are of prime interest from the standpoint of ferroelectricity research may be summarized as follows :

(1) All three phase transitions are microscopically discontinuous. Near the transition points the two adjacent phases coexist.

(2) Considerable changes of the electric field gradient $\triangle E$ at the Nb nucleus occur at the transition points.

(3) The field gradient $\triangle E$ vanishes when the crystal becomes cubic. The equilibrium posistion of the Nb ion probably is in the center of the oxygen octahedron in the unpola- rized phase.

(4) The electric field gradient $\triangle E$ in the polarized phases is too large to be accounted for by a simple ionic model. It appears that at least partial covalent bonding of Nb with O has to be assumed.

Part I : PREPARATION OF SAMPLE

2.2 Preparation of the Samples :

In the present work we aimed to prepare ceramic form of ferroelectric phase of $KNbO_3$, with impurities Ni and Fe doped at different molar concentrations. Ferroelectric ceramics have the advantage of being a great deal easier to prepare than their single crystal. The ceramics system are useful in a variety ways useful for direct technological utility and are regarded to give valuable information about physical mechanisms since being almost like single crystal material.

2.3 The General Formula :

The general formula of our ferroelectrics system is $K(Ni_x Fe_y Nb_z)O_3$ where x+y+z = 1 and x = y = 0.02, 0.05, 0.10 and 0.15.

2.4 Raw-Materials :

A.R. grade Fe_2O_3, NiO, $K_2 CO_3$ and Nb_2O_5 have been used to prepare ferroelectrics.

2.5 Weighing :

The oxides and the carbonates were weighed on a single pan balance with a least count of 10^{-5} gm, and mixed according to their molecular weights.

2.6 Pre-Sintering :

Pre-sintered oxides and corbonates were throughly mixed, finely divided in agate morter in an AR grade acetone base. The mixture was allowed to dry in air, carefully later transferred to a clean dry platinum cruible and sintered in a glo-bar furnace at 700°C for about 8 hours. The samples were cooled, in the furnace at the rate of 80°C per hour by reducing the current gradually. A chromel-alumel thermocouple and digital multimeter were used to measure the temperature. The samples were then finally powdered by grinding in an agate morter.

2.7 Pellet-Formation :

The samples were powdered and pellet of 1 cm diameters were prepared by subjecting them to a pressure of 5 tons/inch^2 for about 10 minutes 10% N solution of polyvinyl aectate was used as the binder.

2.8 Final Sintering :

The pellets thus prepared were final sintered in a glo-bar furnace at 1000°C for about 8 hours. The samples were then cooled at the rate of 80°C/hour.

2.9 Control of Porosity :

One of the aims of ceramic technique is to achieve the lowest possible porosity in the product. This is possibly

made by promoting the sintering rate by using powders with large surface area. Also for this reason the wet chemical preparation method such as co-precipitation are more preferred. The theoretical and experimental studies on sintering process in oxide materials done by Reijnen, (6) showed that the microstructure with large pores is related to compounds having intrinsically a low sintering rate.

Thus the combination of low porosity and small uniform grain size is difficult to obtain by the normal ceramic process. For this pressing of the sample, during the sintering is necessary. It also promotes the sintering process. Hence, hot pressing and continuous hot pressing techniques, are generally preferred. It is very gratifying to note that our ceramic method of preparation yielded samples with considerably low porosity.

Part - II : X-RAY DIFFRACTION STUDY

2.10 The Structure of Perovskite-Type Ferroelectrics :

The perovskite-type ferroelectrics have the paraelectric phase above $415^{o}C$, the cubic unit cell of which is shown Fig.2.1. The space group is O_h-m 3m. Placing the orign at an A ion the atomic co-ordinates are specified as follows :(5)

K   at   0,0,0;

Nb   at   1/2, 1/2, 1/2;

3 O   at 1/2. 1/2, 0; 0,1/2; 1/2; 1/2,0,1/2;

Wood (3) suggested that below the curie point, the atoms are displaced from their original symmetric positions along one of the [001] axes. The structure becomes tetragonal, with the cell dimensions $a = 4.000^{o}A$ and $c = 4.07^{o}A$ as show in Fig.2.2. The space group is 4mm and one formula-unit exists per unit cell. The co-ordinates of the atoms in this structure can be expressed in terms of three parameter δZ_{Nb}, δZ_{OI}, δZ_{OII} representing the shifts of atoms from the symmetrical position, thus,

K at (0,0,0)

Nb at $(1/2,1/2,1/2 + \delta Z_{Nb})$

OI at $(1/2,1/2, \delta Z_{OI})$

2 OII at $(1/2,0\ 1/2 + \delta Z_{OII})$, $(0,1/2,1/2 + \delta Z_{OII})$

The orthombic unit cell is thus approximately twice as large as the simple cubic cell and contains two formula-units. The space group, is C_{2v} mm. The atomic position can be described in terms of displacement of the atoms from the symmetrical position in the cubic phase. The structural problem involves four positional parameters, namely δx_{Nb}, δx_{OI} , δO_{II} and δO_{III} as shown schematically in Fig.2.3.

2.11 X-ray Diffraction Studies

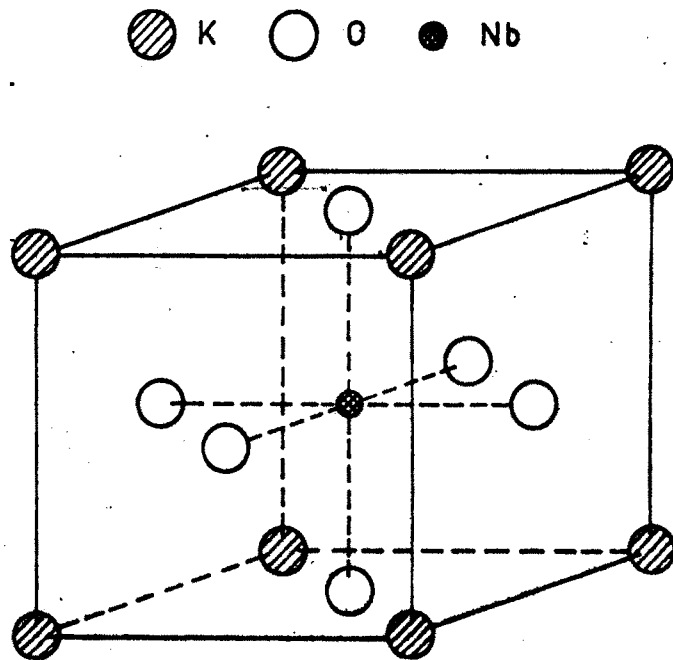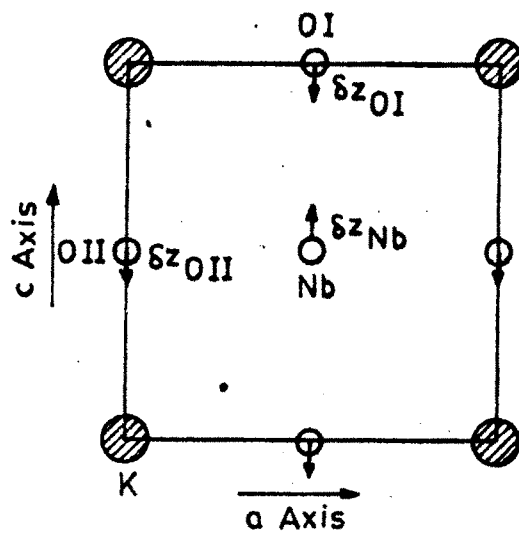In present study an attempt has been made to determine the lattice structure parameters of polycrystalline potassium
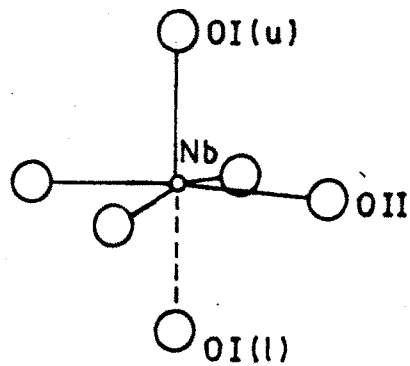
Fig. 2·1 –
Cubic perovskite-type
structure $KNbO_3$.

OI

δz_{OI}

c Axis

OII δz_{OII}

δz_{Nb}

Nb

K

a Axis

(b)

OI(u)

Nb

OII

OI(l)

Fig.2·2− (a)
Structure of tetragonal KNbO$_3$
 (a) Distortion of the NbO$_6$
octahedron.(b) Schematic
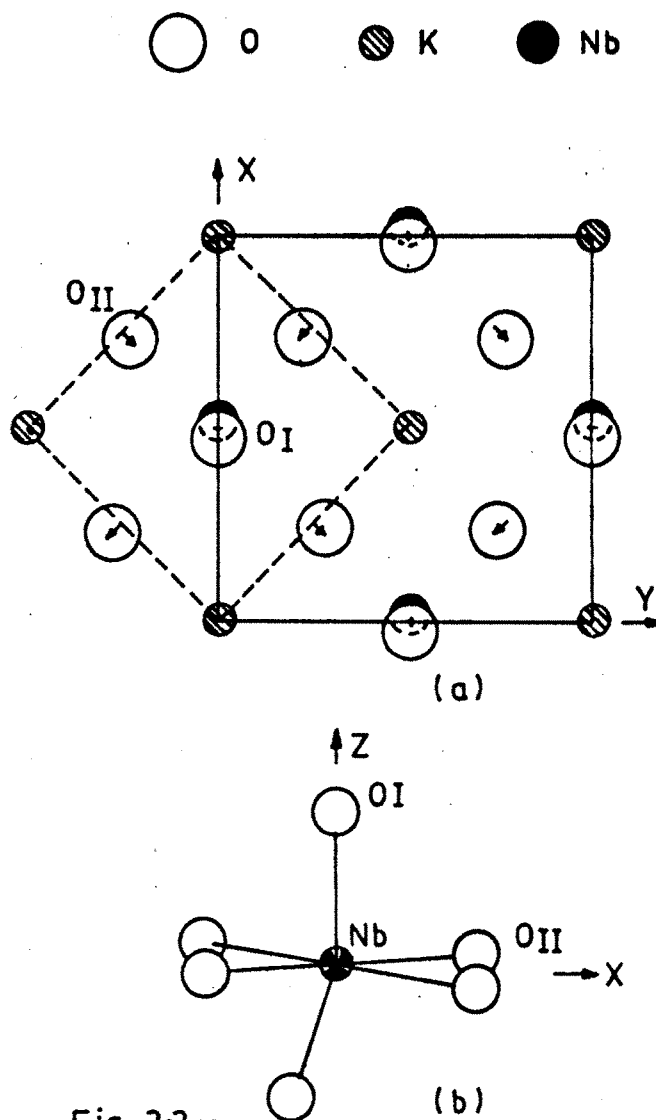projection on (010).

○ O   ◍ K   ● Nb

(a)

(b)

Fig. 2·3 –

Structure of orthorhombic KNbO₃

(a) Schematic projection on orthorhombic (001) plane. (b) Distortion of the NbO₆ octahedron.

niobate ($KNbO_3$) and of the systems $K(Ni_x Fe_y Nb_z)O_3$ ($x = y = 0.02, 0.05, 0.10, 0.15$). Powder diffraction patterns are shown in Fig.2.5 to 2.9. The specifications are as follows :

    (a) Target used   : Fe K_α

    (b) Wavelengths   : 1.93604, 1.9399°A

    (c) Rage of 2θ : 10° to 100°

    (d) Operating voltage : 35kv

    (e) Operating current : 20mA.

2.12 Crystal Structure Characterisation

The interplanar distance d_{hkl} , the lattice parameter a,b,c and the indices hkl can be related for a orthorhombic as

$$d_{hkl} = \frac{1}{\sqrt{h^2/a^2 + k^2/b^2 + l^2/c^2}} \qquad (2.1)$$

The combination of this relation with the Bragg's law

$$Sin^2 \theta_{hkl} = \lambda^2/4 \left[h^2/a^2 + k^2/b^2 + l^2/c^2 \right] \qquad (2.2)$$

$$Sin^2 \theta_{hkl} = A h^2 + B k^2 + C l^2 \qquad (2.3)$$

where $A = \lambda^2/4a^2$, $B = \lambda^2/4b^2$ $C = \lambda^2/4c^2$.

The greatest common factor (GCF) was determined from a few lines at the lower angles and then all the other proper integers were found. Taking into consideration three hkl values, the lattice parameters a, b, and c are determined

from (GCF). The d_{hkl} values were calculated using (2.1) for J_1 to J_5 samples. The proper selection, among the hkl values and lattices constant a, b, and c was made till the observed and calculated d_{hkl} values suit in closest agreement.

2.13 Results and Discussion

The calculated d values of these samples and the other were found in close agreement with their respective observed d value. The lattice parameters a,b, and c were determined for all the samples studied.

The compositional variation of the lattice parameters a,b, and c for the ferroelectric systems of $KNbO_3$ with the impurities Ni and Fe is shown in Fig.2.4. It is seen that, as the impurities concentration increased, the lattice parameters also increase. All the parameters are found maximum for the impurity x = y = 0.05 sample. Then the parameters are found to decrease with the increase in the impurty concentration.

The lattice parameters of $KNbO_3$ reported earlier by the other authors and as well the present work data are summerized in Table.2.2. They are in reasonably good agreement.

Table 2.2 : Lattice parameters of $KNbO_3$

	$a^{\circ}A$	$b^{\circ}A$	$c^{\circ}A$
(1) Wood (3)	3.984	5.702	5.739
(2) Shirane et al (1)	3.973°	5.695	5.721
(3) Present work			
J_1	3.9663	5.6548	5.7120
J_2	3.9687	5.6548	5.7112
J_3	3.9805	5.6656	5.7266
J_4	3.9729	5.6578	5.7124
J_5	3.9394	5.6312	5.6512

2.14 Porosity in $K(Ni_x Fe_y Nb_z)O_3$ Ferroelectric System

Knowing the molecular weight and the lattice constants, the X-ray densitiy of each sample was evaluated with the help of following equation

$$\rho_x = \frac{\text{molecular weight} \times \text{no.of molecular per unit cell}}{\text{volume of unit cell} \times 6.022 \times 10^{23} \text{ molecules/mole}} \quad (2.3)$$

The use of measured physical density (ρ_s) of a sample, along with its X-ray density was made to evaluate the percentage of porosity in a sample. We know that,

$$\text{porosity } \% = \frac{\rho_x - \rho_s}{\rho_x} \times 100.$$

The X-ray and physical densities along with the porosity % of all the $K(Ni_x Fe_y Nb_z)O_3$ ferroelectric system are listed in Table.2.3.

Table 2.2 : The crystallographic data of $K(Ni_x Fe_y Nb_z)O_3$ -ferroelectrics.

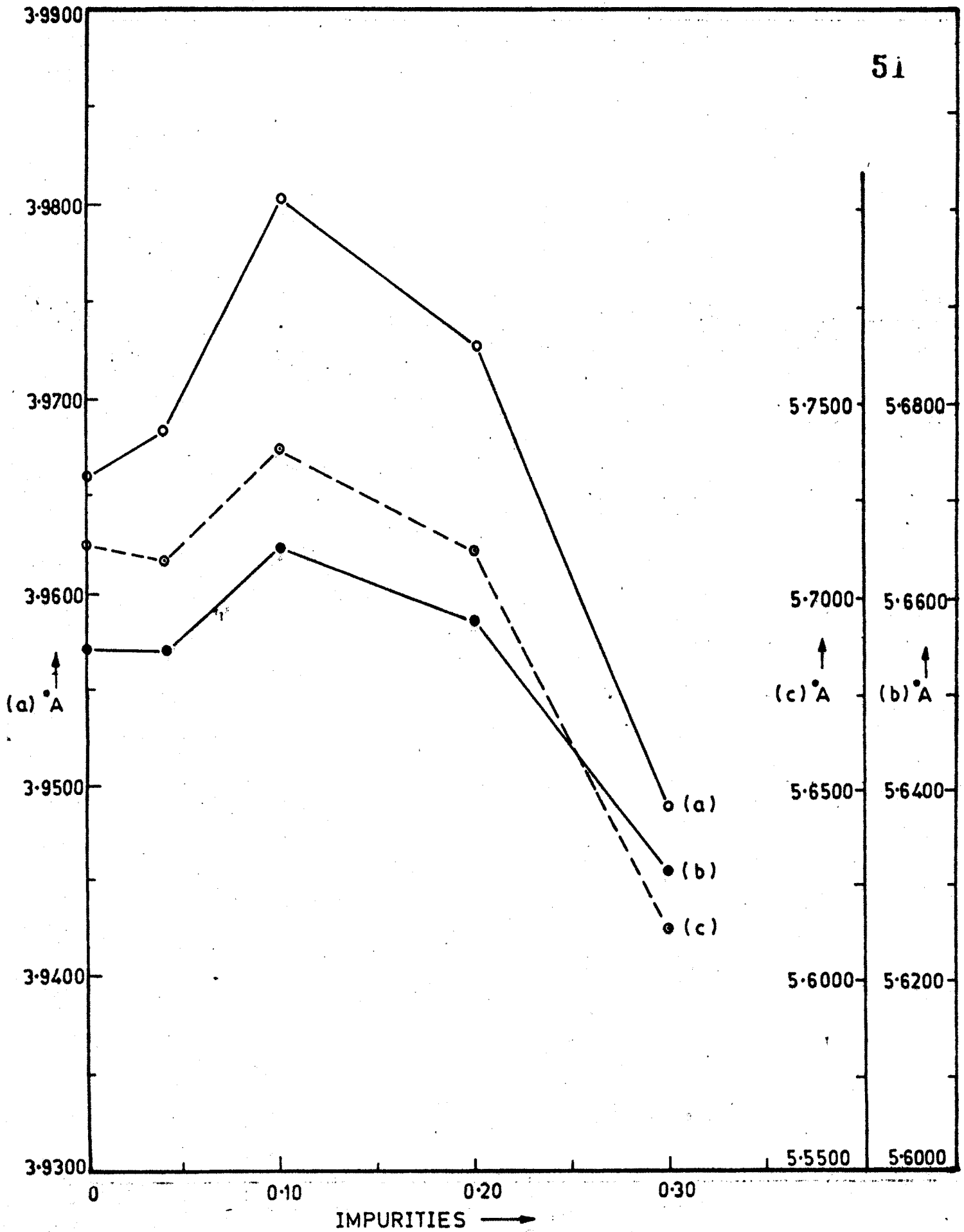| Sample	Composition	Lattice parameters			X-ray density ρ_x(gmcm^{-3})	Physical density ρ_s(gm cm^{-3})	Porosity % $\dfrac{\rho_x-\rho_s}{\rho_s} \times 100$
		a°A	b°A	c°A			
J_1	$KNbO_3$	3.9663	5.6548	5.7120	5.6192	4.898	14.7
J_2	$K(Ni_{0.02}Fe_{0.02}Nb_{0.96})O_3$	3.9687	5.6548	5.7112	5.5716	4.3743	21.48
J_3	$K(Ni_{0.05}Fe_{0.05}Nb_{0.90})O_3$	3.9805	5.6656	5.7266	5.4638	4.928	10.0
J_4	$K(Ni_{0.1}Fe_{0.1}Nb_{0.80})O_3$	3.9729	5.6578	5.7174	5.3844	4.339	17.6
J_5	$K(Ni_{0.15}Fe_{0.15}Nb_{0.70})O_3$	3.9494	5.6312	5.6512	5.1014	4.522	19.7

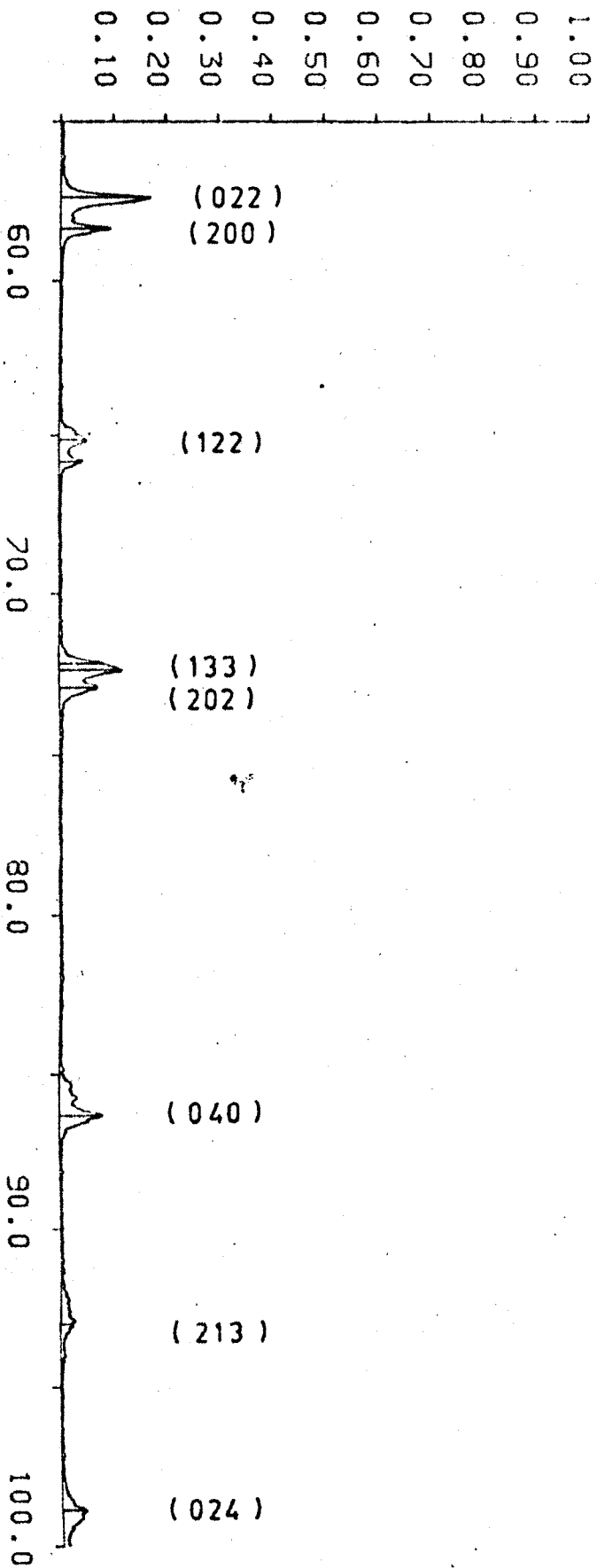Fig. 2·4 – THE COMPOSITIONAL VARIATION OF THE LATTICE PARAMETERS a, b AND c WITH THE IMPURITIES.

52

x10³

1.00
0.90
0.80
0.70
0.60
0.50
0.40
0.30
0.20
0.10

1.00
0.90
0.80
0.70
0.60
0.50
0.40
0.30
0.20
0.10

10.0

20.0

0.0

40.0

50.0

(011)
(100)

(002)
(020)

(102)

60.0

70.0

80.0

90.0

100.0

(022)
(200)

(122)

(113)
(202)

(004)
(040)

(104)
(213)

(024)

×10³

(022)
(200)

(122)

(133)
(202)

(040)

(213)

(024)
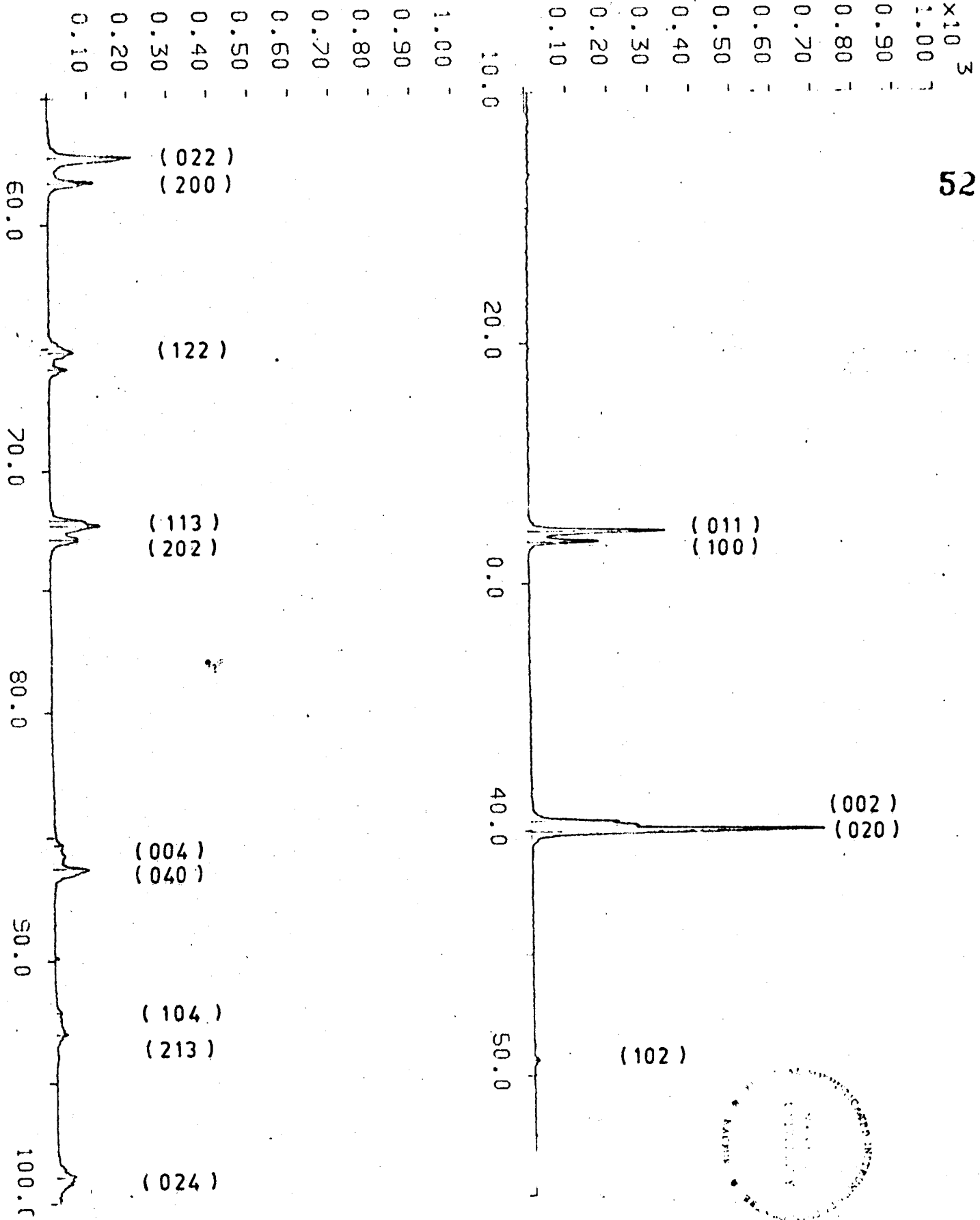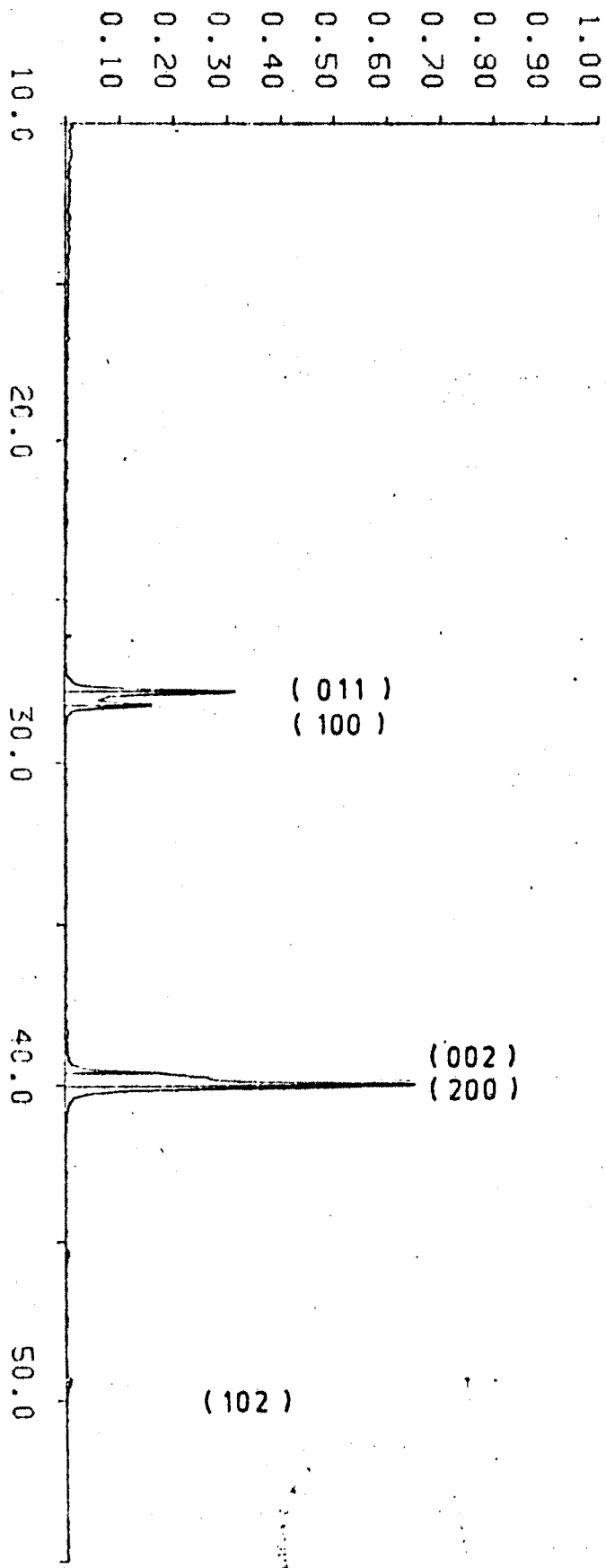
Fig. 2·6: X-RAY DIFFRACTION PATTERN OF K (Ni₀.₉₃Fe₀.₀₇Nb₀.₀₆)O₃

(011)
(100)

(002)
(200)

(102)

Fig.7.7: X-RAY DIFFRACTION PATTERN OF K(Ni₀.₀Fe₀.₀Nb₀.₀₀)O₃

Fig.7.8: X-RAY DIFFRACTION PATTERN OF K(Ni₀.₀Fe₀.₀Nb₀.₀)O₃

(022)
(200)

(122)

(220)
(202)

(113)
(040)

(213)

(024)

(010)
(100)

(020)
(200)
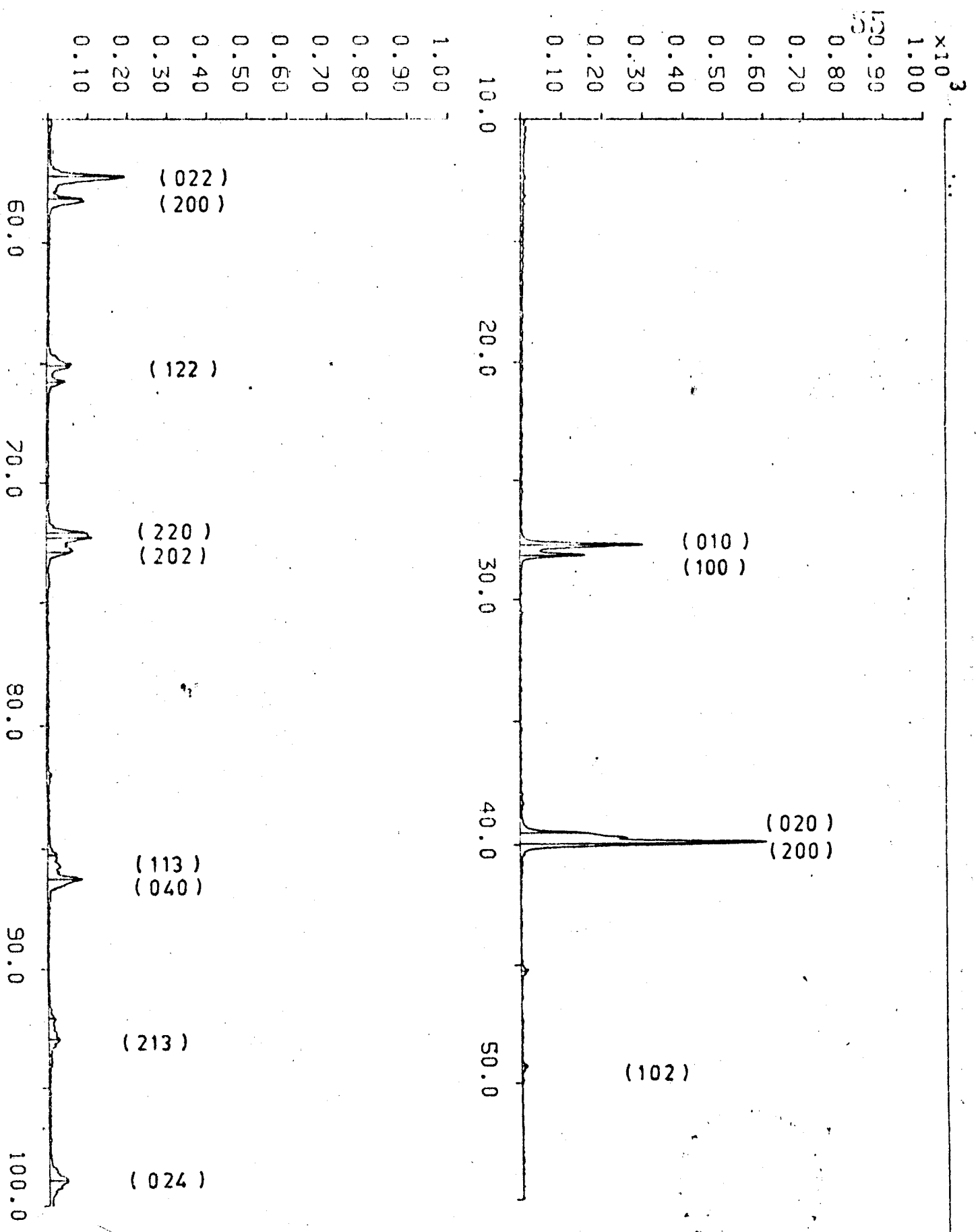
(102)
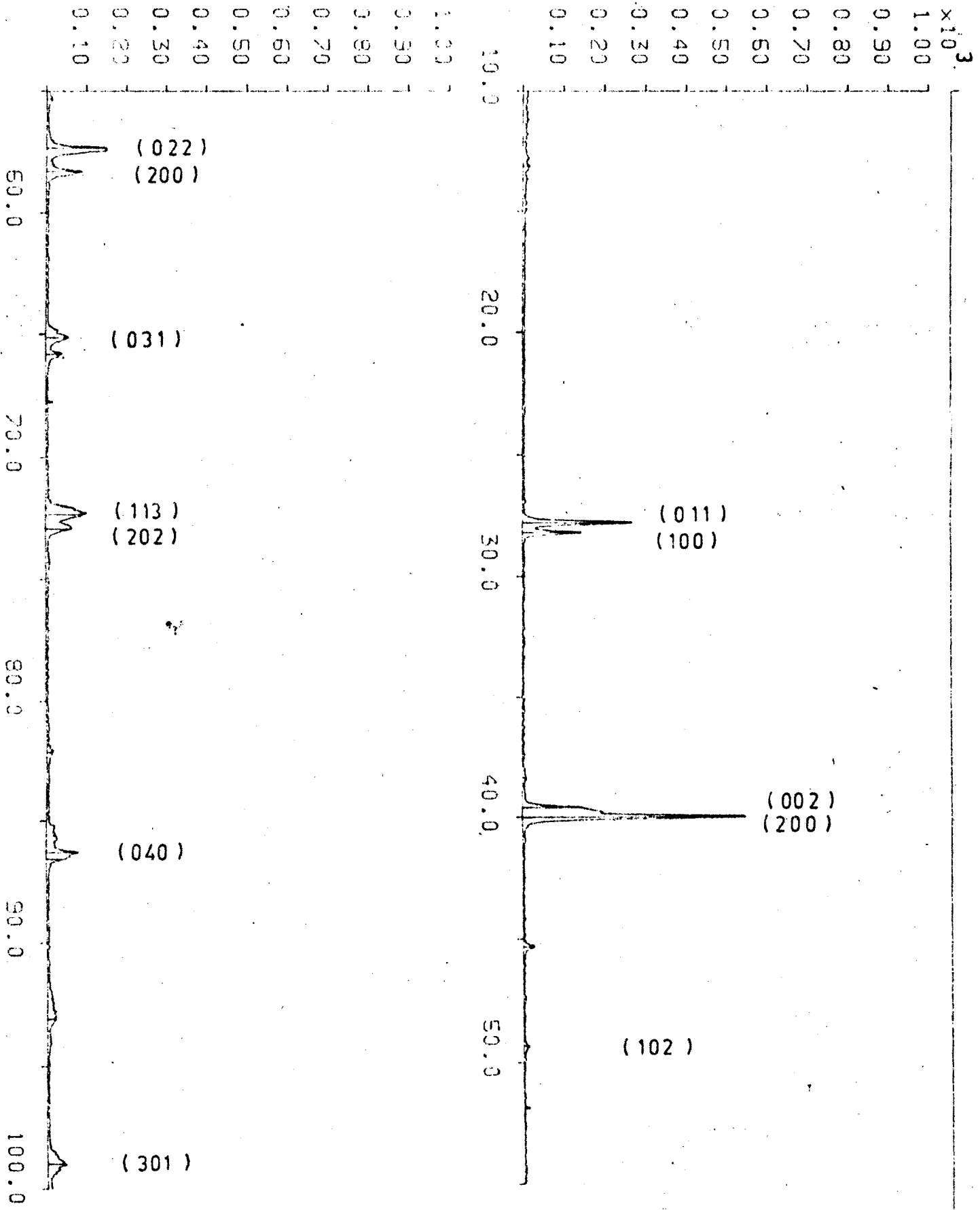
Fig. 2·9: X-RAY DIFFRACTION PATTERN OF K (Ni$_{0.15}$ Fe$_{0.15}$ Nb$_{0.70}$) O$_3$.

R E F E R E N C E S

1) Shirane, G.   (1954) Phys.Rev. 93, 672.
   Danner, H.
   Pavlovic, A. and
   Pepinsky, R.

2) Shirane, G.   (1954) Phys.Rev. 96, 581.
   Newnham, R. and
   Pepinsky, R.

3) Wood, E.A.   (1951) Acta Cryst. 4, 353.

4) Matthias, B.T.   (1951) Phys.Rev. 82, 727.
      and
   Remeika, J.P.

5) Ewald, P.P. and (1931) Structurbericht, 1913-28.
   Herman, C.   Leipzig :Akademische Verlagsgesellschaft.

6) Reijnen, P.J.L. (1968) Sci.Ceram. 4, 169.

7) Cotts, R.M. and (1954) Phys.Rev. 96, 1285.
   Knight, W.D.